Tuning the efficient blue/red afterglow in a luminescent plastic film

YANAN ZHU[1,2,*#], LIUBING ZHENG[1,2#], ZENGHUI RAO[1,2#], RADHIKA VAID[3], ZENGYUAN PANG[1,2], MINGQIAO GE[1,2], DEKANG GAO[4]

[1]*College of Textile Science and Engineering, Jiangnan University, Wuxi, Jiangsu 214122, China*
[2]*Key Laboratory of Eco-Textiles, Ministry of Education, Jiangnan University, Wuxi, Jiangsu 214122, China*
[3]*Wilson College of Textiles, North Carolina State University, 1020 Main Campus Drive, Raleigh, 27606, USA*
[4]*Bosideng International Holding Co., Ltd., Changshu, Jiangsu, 215532, China*
[#]*Yanan Zhu, Liubing Zheng and Zenghui Rao contributed equally to this work*

Light quality, especially of red and blue light, has been considered a crucial concern which dictates numerous adaptive responses and determines the developmental transitions in plants. During the research, one easy and efficient strategy is demonstrated to replenish red and blue light for extended durations through a luminescent plastic film, which is prepared using a composite luminescent material ($Sr_2MgSi_2O_7$:Eu^{2+}, Dy^{3+}/light conversion agent). This composite material refers to certain type of long afterglow luminescent material fabricated using a combination of a light conversion agent and $Sr_2MgSi_2O_7$:Eu^{2+}, Dy^{3+} with the given mass ratio. $Sr_2MgSi_2O_7$:Eu^{2+}, Dy^{3+}, when excited under UV light and near-UV light for a short time, can emit blue light for more than eight hours. It also serves as kind of blue persistent luminescence donor phosphor. In addition, the light conversion agent has been applied in tuning blue light to red light partially as the red conversion phosphor. The red/blue light ratio can be controlled by varying the doping content of the light conversion agent and $Sr_2MgSi_2O_7$:Eu^{2+}, Dy^{3+} taking into account the different needs of plants.

(Received September 28, 2021; accepted April 7, 2022)

Keywords: Luminescent film, Red/blue light, Composite materials, Light conversion agent, $Sr_2MgSi_2O_7$:Eu^{2+}, Dy^{3+}

Light quality is playing an important part in determining the numerous adaptive responses. It also helps in the development transitions in plants. Growth and physiology of plants suffer from intense influences of blue color and red color [1–3]. Red light promotes leaf morphogenesis, the formation of photosynthesis mechanisms, and carbohydrate accumulation mainly through the participation of phytochrome [4]. Blue light, mediated by cryptochrome and phototropin, is playing a vital part in photosynthesis, chlorophyll formation, and stomata opening [5,6]. A study on the effect of light quality on seedling morphoanatomy and physiology for *Campomanesia pubescens* (DC.) O. Berg. indicated that increased stomatal density and stomatal functionality resulted in the generation of relatively high leaf and stem dry mass in case that seedling growth is under the influence of white and blue/red lights [7]. Further research was conducted to understand the response of Brassicaceae microgreens-related yield and appearance quality to different blue light ratios in red and blue light-emitting diodes. The results indicated response of plants to blue light relies on plant traits as well as microgreen species. It was also observed that it is important to regulate the ratio of red to blue light for reaching an equilibrium between yield and appearance quality [8]. In addition, a study on the nitrate content in *Valerianella locusta* (L.) plants grown under the influence of supplemental LED lighting indicated nitrate content reduced sharply in lettuce of lambs growing in 90% red + 10% blue LED light. The nitrate content was lower than the nitrate content in plants treated under the influence of high-pressure sodium lamps [9]. Moreover, an interesting study conducted on the red light syndrome revealed that blue light relieved “red light syndrome” through adjusting chloroplast ultrastructure, photosynthetic properties, as well as nunutrient accumulation for the cucumber plant [10].

Light has been considered a major environmental factor influencing the growth and development regulation in plants. In addition, it is important to supplement and adjust the light quality for realizing effective plant growth and development. Therefore, colorful plastic films have been widely used in plant culture. Different colored plastic films provide different qualities of light to plants [11–13]. A study on the effect of colored light-quality selective plastic film on anthocyanin content, enzyme activity, as well as flavonoid gene expression of strawberry fruits had been performed. The result showed that red and yellow light-quality selective plastic film treatments can potentially help supplement the cultivation practice to enhance anthocyanin contents of growing strawberry fruits [14]. According to a similar survey concerning the impact of colored plastic film on photosynthetic properties as well as active ingredient contents in *Dysosma versipellis*, it was suggested that blue film treatments of *D. versipellis* facilitate photosynthesis as well as podophyllotoxin accumulation [15]. Further, the effects of red and blue light on the morphology and flowering capability in *Petunia* × *hybrida* had been examined. The results

indicated different impacts on the morphology and flowering capacity in *Petunia* × *hybrida* in different seasons [16]. The reported results indicated that colored plastic film was useful in management through generating particular light spectra. However, the colored plastic film does not work in the absence of artificial light sources at night.

To address this gap, the present study reports the effects of red/blue luminescent films doped with composite luminescent material, $Sr_2MgSi_2O_7:Eu^{2+}$, Dy^{3+}/light conversion agent on plants. $Sr_2MgSi_2O_7:Eu^{2+}$, Dy^{3+}/light conversion agent is a long afterglow luminescent material fabricated from a combination of light conversion agent and $Sr_2MgSi_2O_7:Eu^{2+}$, Dy^{3+} [17–20]. It exhibits outstanding properties, including high brightness as well as good stability of $Sr_2MgSi_2O_7:Eu^{2+}$, Dy^{3+}. Thus, it can absorb UV and visible light within several minutes, and emit blue light for over eight hours. At the same time, it exhibits light conversion characteristics, which is effectively activated by light with a spectrum scope in UV - 500 nm and releases red light [21–23]. Thus, the luminescent films can not only provide plants a certain amount of red and blue light but also emit blue/red light at night, even in the absence of artificial light sources. In addition, the red/blue light ratio can be controlled by adjusting the doping content in composite luminescent materials.

1. Experimental

1.1. Materials

$SrCO_3$ (A.R.), MgO (A.R.), SiO_2 (A.R.), Eu_2O_3 (99.99%), Dy_2O_3 (99.9%), H_3BO_3 (A.R.), C_2H_6OS (dimethyl sulfoxide, DMSO), and light conversion agent ($C_{28}H_{29}O_3N_2Cl$) were provided by Sinopharm Chemical Reagent Co., Ltd., China. Silane coupling agent came from Shanghai Guo Yao Group Chemical Reagent Co., Ltd. Aluminate coupling agent came from Nanjing Daoling Chemical Co., Ltd. Aluminum zirconium coupling agent came from Yangzhou Lida Resin Co., Ltd. Polyacrylonitrile (PAN) (Mw = 150,000 g/mol) was provided by Sigma-Aldrich.

1.2. Preparation of $Sr_2MgSi_2O_7:Eu^{2+}$, Dy^{3+}

$Sr_2MgSi_2O_7:Eu^{2+}$, Dy^{3+} was produced through solid-state reaction with analytical reagent (A.R.) grade $SrCO_3$, MgO, Eu_2O_3, Dy_2O_3, and H_3BO_3 as raw materials. $SrCO_3$, MgO, Eu_2O_3, Dy_2O_3, and H_3BO_3 were precisely weighed with specific measurement ratio stipulated by $Sr_{1.94}MgSi_2O_7$, $0.02Eu^{2+}$, $0.04Dy^{3+}$, and $0.1B^{3+}$. Then measured materials were stored by the mortar, followed by grinding and mixture for 30 min, and finally poured into one small beaker. Afterwards, the mixture was dissolved by absolute ethanol in a proper amount. Subsequently, the mixture was subjected to conditions of ultrasonic dispersion for 30 min for preparing the homogeneous mixture. Resulting hybrid was dried at 80 °C, and then milled by using the crucible. The crucible was subsequently positioned inside the high-temperature tube sintering furnace, being heated at 1400 °C for 4 h in the reducing environment. Finally, sintered products needed to be ground and screened for obtaining the required samples.

1.3. Preparation of $Sr_2MgSi_2O_7:Eu^{2+}$, Dy^{3+}/light conversion agent

$Sr_2MgSi_2O_7:Eu^{2+}$, Dy^{3+}, light conversion agent, and deionized water were introduced to the breaker, with continuous stirring for 30 min. Following this, the coupling agent (the content of silane, aluminum zirconium, and aluminate was 1.25%) was added to the mixture under conditions of stirring and heating. A water bath was used to heat the mixture for 30 min in the temperature range of 40 °C – 50 °C. Ultrasonic treatment was subsequently performed for 15 min (frequency: 100 kHz). Afterwards, samples were blended and heated at 60 °C – 70 °C till complete evaporation of deionized water. Then all samples needed to be positioned inside an oven, for being heated at 70 °C for 2 h. Ultimately, driedproducts were ground and screened for obtaining required samples.

1.4. Preparation of luminescent films

PAN and DMSO were precisely weighed with mass ratio of 19:100, and then introduced into one beaker. The mixture was continually blended and heated in water bath. Heating temperature fell into the scope of 60 °C – 70 °C. All samples were heated for 4 h for preparing PAN film-forming polymer. Composite luminescent materials were introduced to PAN film-forming polymer and stirred until a homogenous dispersion was obtained. The polymer and composited luminescent material blend were then poured into one round mold about 2 cm in diameter and 1mm thick. Luminescent films were prepared when the mold was immersed with deionized water at 20 °C for 30 min. The ratios of the doped composite luminescent material to PAN film-forming polymer were 3%, 5%, 7%, 9%, 11%, and 13%.

1.5. Scanning electron microscopy (SEM)

For investigating the microstructure in $Sr_2MgSi_2O_7:Eu^{2+}$, Dy^{3+}/light conversion agent of luminescent film, luminous film cross-section was examined with the SEM (Quanta200, the Netherlands) technology and corresponding voltage increased to 20 kV. The samples needed to be dried and coated with gold before scanning.

1.6. X-ray diffraction (XRD)

XRD patterns could be documented using the D8 Advance X-ray diffractometer (Bruker AXS, Germany)

with Cu Kα radiation (λ= 0.15406 nm) when the voltage was 40 kV and the current was 30 mA. All samples had scanning in 2θ scope of 5°–90°, and corresponding scanning rate was 0.1(°)/s at ambient temperature.

1.7. Luminous properties

Excitation and emission spectra were recorded, and photon conversion efficiency of all samples was calculated with the fluorescence spectrophotometer (HITACHI650–60, Japan), where the inbuilt Xe flash lamp served as the excitation source. Relevant experiments were conducted at room temperature (scan speed: 120 nm/min). Chromaticity coordinates were checked. Chromaticity diagrams were plotted with one fluorescence spectrophotometer. The afterglow decay curves could be investigated with one PR-305 afterglow brightness tester (excitation illumination: 1000 lx, excitation time: 15 min) at ambient temperature. All samples needed to be stored in a dark environment for over 15 h before test, thus ensuring afterglow illumination had been totally faded. Digital photos for overall samples had been captured by one single-lens reflex camera, in which its inbuilt Xe flash lamp served as the excitation source.

2. Results and discussion

2.1. Schematic energy level diagrams

The luminescent plastic film is demonstrated in Fig. 1. From Fig. 1, the critical role played by light conversion agent and $Sr_2MgSi_2O_7:Eu^{2+}$, Dy^{3+} can be depicted when rendering plastic film luminous. Among these two functional materials, the luminescent plastic film can emit light in the range of 400-700 nm, which is good for the development of plants.

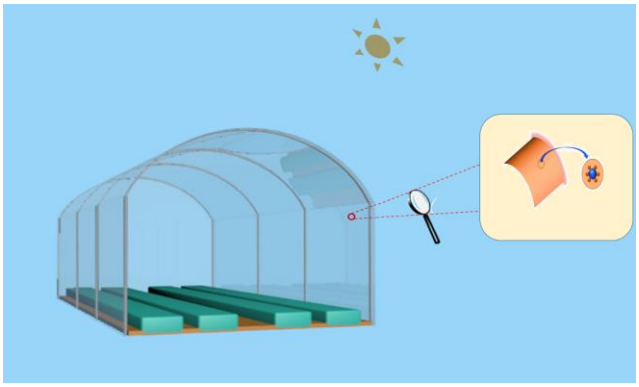

Fig. 1. Schematic diagram of the luminescent plastic film (color online)

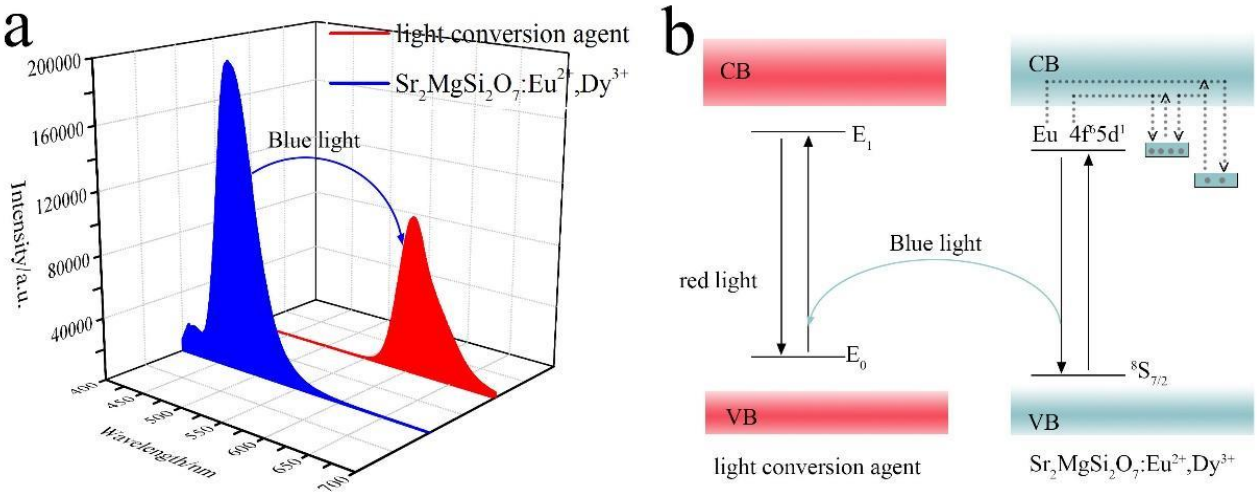

Fig. 2. Possible afterglow mechanism of the composite luminescent material $Sr_2MgSi_2O_7:Eu^{2+}$, Dy^{3+}/light conversion agent (color online)

The potential afterglow mechanism related to composite luminescent material $Sr_2MgSi_2O_7:Eu^{2+}$, Dy^{3+}/light conversion agent, is illustrated in Fig. 2. Under conditions of UV light excitation, the ground-state electrons in Eu^{2+} ions were excited to conduction band (CB). Excited electrons were then captured by electron traps from CB. During an ever-lasting luminescence process, those electrons captured by shallow traps escape thermally through CB and have recombination with Eu^{2+}. The process may occur with long and ensuring blue luminescence. Thereafter, the blue light pumped the photoluminescence of the light conversion agent. Such light conversion agent can be considered one small organic particle having plenty of conjugated structures. Ground-state electrons in such conjugated structures were stimulated to be in the exited state when being exposed to blue light. Red light occurred in condition that electrons recovered to the ground state.

2.2. SEM analysis

Fig. 3 exhibits sample SEM images. The description of the digital images of the luminescent PAN films has also been presented. Particles in $Sr_2MgSi_2O_7:Eu^{2+}$, Dy^{3+} and light conversion agent of an irregular shape can be observed in Figs. 3 (a), (b), (c), and (d). It is revealed that the particles of $Sr_2MgSi_2O_7:Eu^{2+}$, Dy^{3+} in Fig. 3 (b) are larger than that of the light conversion agent of Fig. 3 (c). Particle size in $Sr_2MgSi_2O_7:Eu^{2+}$, Dy^{3+} was approximately 10–15 microns, and the particle size of the light conversion agent was approximately 1–2 microns. Thus, it is feasible to coat the light conversion agent onto $Sr_2MgSi_2O_7:Eu^{2+}$, Dy^{3+} surface when preparing composite luminescent material. The observations made during the coating for $Sr_2MgSi_2O_7:Eu^{2+}$, Dy^{3+} with the light conversion agent are illustrated by Fig. 3 (a). $Sr_2MgSi_2O_7:Eu^{2+}$, Dy^{3+} surface was rougher than that presented in Fig. 3 (b) because it was fixed onto particles in the light conversion agent through a coupling agent used as an intermediate combination agent. Fig. 3 (e) depicts the structure of the luminescent film based on the results obtained from the analysis of the digital image, where the composite luminescent materials exist on the internal surface of luminescent film, though the particles in $Sr_2MgSi_2O_7:Eu^{2+}$, Dy^{3+} and light conversion agent are visible. The particles of light conversion agent seem well dispersed across the film. The large white particles correspond to $Sr_2MgSi_2O_7:Eu^{2+}$, $Dy^{3+,}$ while those small red ones correspond to light conversion agents. Moreover, white particles are capable of absorbing and storing sunlight and subsequently emitting blue light, and small red particles are capable of transforming blue light to red light partially. As a result, red and blue lights are provided to plants. The luminescent film appears red because a large number of the particles corresponding to the red light conversion agent are distributed inside the luminescent film.

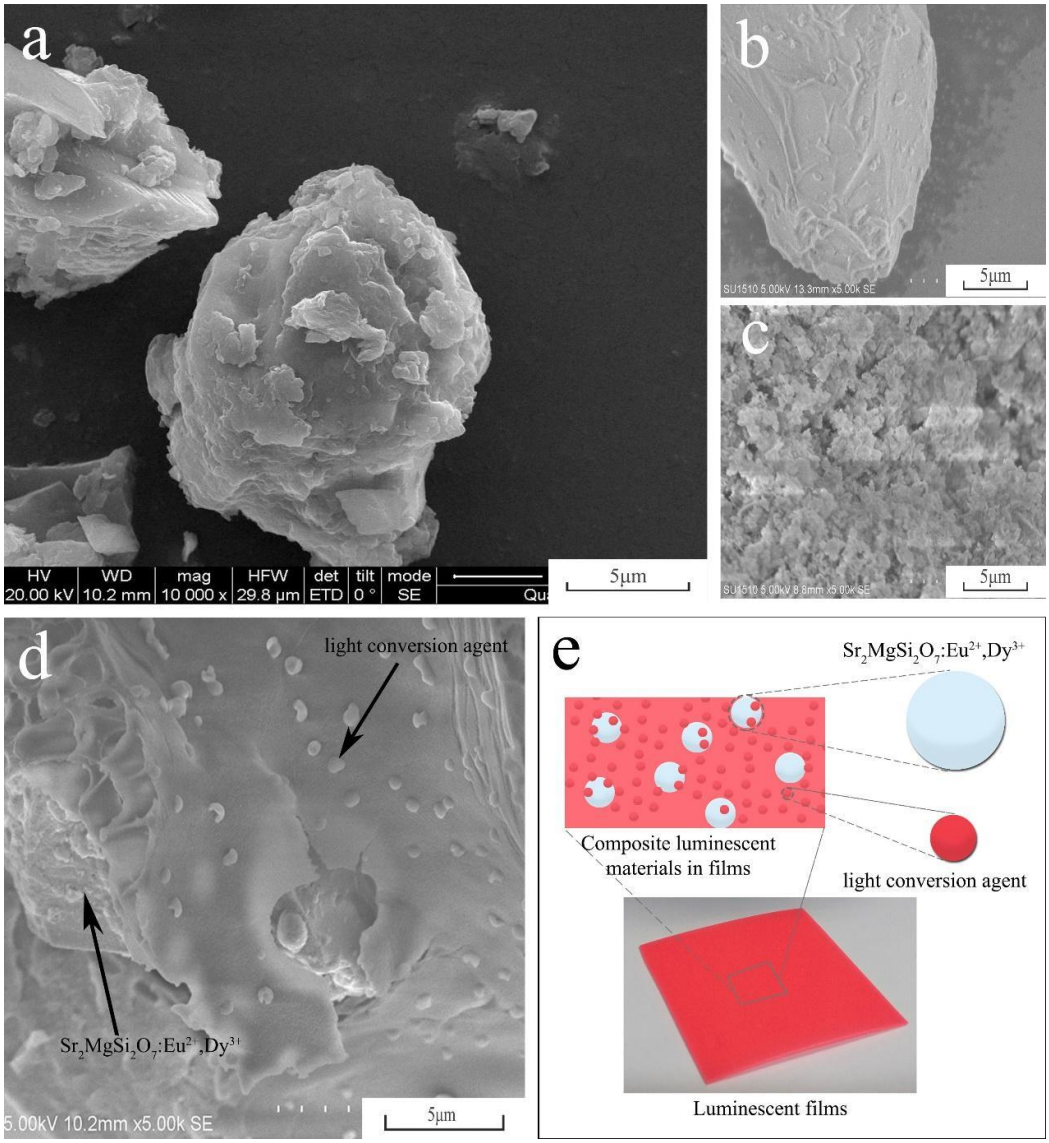

Fig. 3. Scanning electron microscopy images of samples and description of the digital images of samples. (a) Composite luminescent materials, (b) $Sr_2MgSi_2O_7:Eu^{2+}$, Dy^{3+}, (c) Light conversion agents, (d) Luminescent films. (e) Description of the digital images of the luminescent films fabricated with composite luminescent materials (color online)

2.3. XRD analysis

XRD measurements of luminescent films were performed for analyzing the crystal matrix in luminescent film. According to Fig. 4, pure monoclinic diffraction peaks in luminescent film were dominated by XRD patterns that much resembled those recorded for the commercially available $Sr_2MgSi_2O_7:Eu^{2+}$, Dy^{2+} phosphors. XRD patterns related to luminescent film occur when sharp peaks are at 17°, 28.5°, 30.7°, 35.8°, and 43.5° 2θ, which correspond to characteristic diffraction peaks in $Sr_2MgSi_2O_7:Eu^{2+}$, Dy^{3+}. As proved by above results, these complicated fabrication processes and light conversion agent doping had no destructive impacts on the $Sr_2MgSi_2O_7:Eu^{2+}$, Dy^{3+} phase of the film. In addition, the position and shape of diffraction peaks that corresponded to luminescent films that contain different amounts of luminescent materials remained unchanged, although the intensity of the luminescent films with different contents of luminescent materials changed.

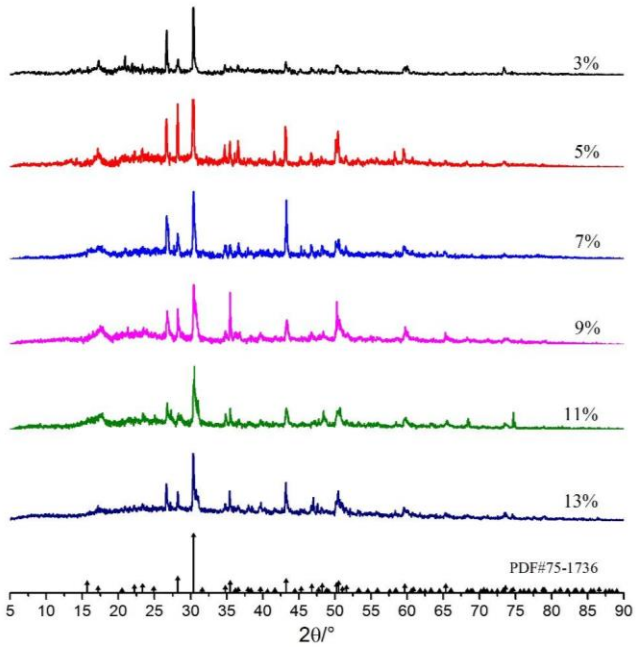

Fig. 4. XRD patterns for luminescent film having luminescent materials with varying doping ratios and PDF card no. 75–1736 (color online)

2.4. Spectrum analysis

Relevant analytical results on the excitation and emission spectra for $Sr_2MgSi_2O_7:Eu^{2+}$, Dy^{3+} and light conversion agent of Figs. 5(a) and (b) indicate that $Sr_2MgSi_2O_7:Eu^{2+}$, Dy^{3+} may be effectively stimulated by light of wavelength spanning the UV region to 450 nm. They can emit blue light with the maxima at approximately 470 nm. In addition, the light conversion agent may also be effectively stimulated by light of wavelength spanning the UV region to 500 nm. Red light is emitted with a peak at 600 nm. The excitation spectrum perfectly overlaps with the persistent luminescence spectrum for $Sr_2MgSi_2O_7:Eu^{2+}$, Dy^{3+} (across the 430 nm - 550 nm region; peak at around 470 nm). Thus, $Sr_2MgSi_2O_7:Eu^{2+}$, Dy^{3+} can serve as a persistent luminescence donor material for the light conversion agent. Luminescent films were prepared using a PAN film-forming polymer using different amounts of $Sr_2MgSi_2O_7:Eu^{2+}$, Dy^{3+}/light conversion agents as doping materials. Figs. 5 (c) and (d) represent the excitation and emission spectral profiles for luminescent films containing 3%, 5%, 7%, 9%, 11%, and 13% of the luminescent materials. Analysis of Fig. 5 (c) reveals the excitation spectra for luminescent film shows a wide band in the region spanning from UV to 500 nm. Two excitation peaks located at approximately 306 and 356 nm were observed. The emission spectral profiles of the luminescent film were observed with 356 nm as an exciting wavelength, as demonstrated in Fig. 5(b). The figure reveals two emission bands positioned at about 470 and 600 nm, corresponding to blue light and red light, respectively. The emission peak at approximately 470 nm should be ascribed to representative $4f^65d^1–4f^7$ transition of Eu^{2+}. Another peak at around 600 nm should be ascribed to light conversion agent emission that absorbs UV and blue light. Following this, it releases red light. The red/blue ratio (Int. (600 nm) vs. Int. (470 nm)) in the films with varying amounts of luminescent material is used for investigating how doping ratio affects spectral tuning (Fig. 5 (e)). The red/blue ratio increased with an increase in the luminescent material content. Thus, the intensity ratio of the red and blue light released by the film can be adjusted by introducing different percentages of luminescent materials. Fig. 5 (f) shows the quantum yield of the luminescent films containing different percentages of the luminescent material. The scatter integration range was 345 nm to 370 nm, and the emission integration range was 400 nm to 700 nm. The quantum yields of the luminescent films containing 3%, 5%, 7%, 9%, 11%, and 13% of the luminescent materials were 27.1%, 30.6%, 35%, 39.3%, 39.8%, and 46.6%, respectively. The results thus depict that the quantum yield is proportional to the doping content of the luminescent materials.

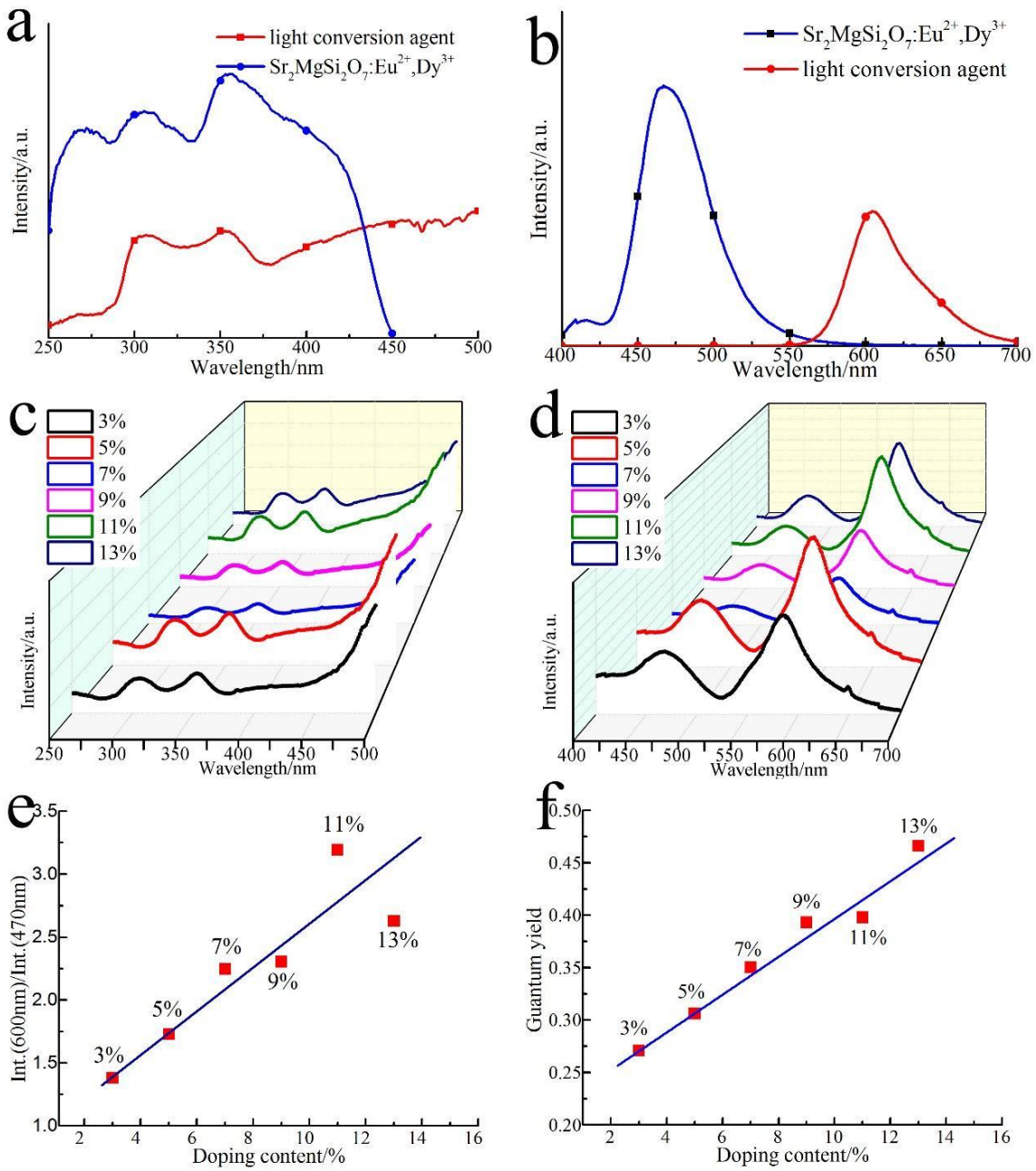

Fig. 5. (a) Excitation spectral profiles of $Sr_2MgSi_2O_7:Eu^{2+}$, Dy^{3+} and light conversion agent. (b) Emission spectral profiles for $Sr_2MgSi_2O_7:Eu^{2+}$, Dy^{3+} and light conversion agent. (c) Excitation spectral profiles of luminescent films with varying amounts of luminescent materials (3%, 5%, 7%, 9%, 11%, and 13%). (d) Emission spectral profiles of the luminescent films with varying amounts of luminescent materials. (e) (Int.(600 nm) vs. Int.(470 nm)) of luminescent films with varying amounts of luminescent materials. (f) Quantum yields for luminescent films with varying amounts of luminescent materials (color online)

2.5. Decay of the afterglow

The initial afterglow brightness in luminescent film containing various composite luminescent material contents and the afterglow decay characteristics of the luminescent films are demonstrated in Figs. 6 (a) and (b), respectively. According to Fig. 6 (a), the afterglow initial brightness in luminescent films containing 3%, 5%, 7%, 9%, 11%, and 13% luminescent materials were 0.076, 0.126, 0.133, 0.142, 0.180, and 0.186 cd/m^2. As luminescent material content increased, the initial afterglow brightness gradually increased. Further, the analysis of Fig. 6 (b) reveals that the afterglow decay in luminescent film can be observed. The decay process comprising one quick attenuation step (first 300 s) followed by one slow decay step. The finding should be attributable to the trap levels at various depths inside the luminescent material.

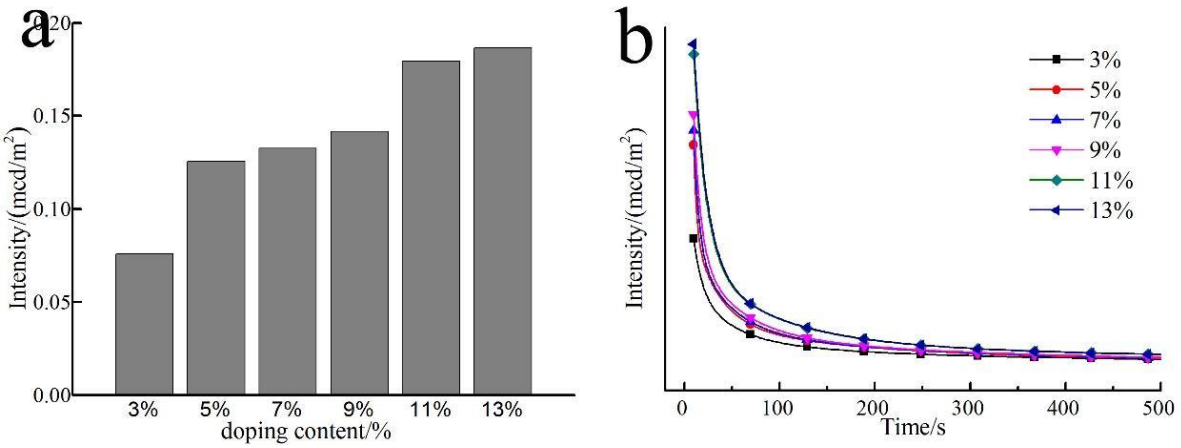

Fig. 6. (a) Afterglow initial brightness in luminescent films. (b) Afterglow attenuation diagram of the luminescent films (color online)

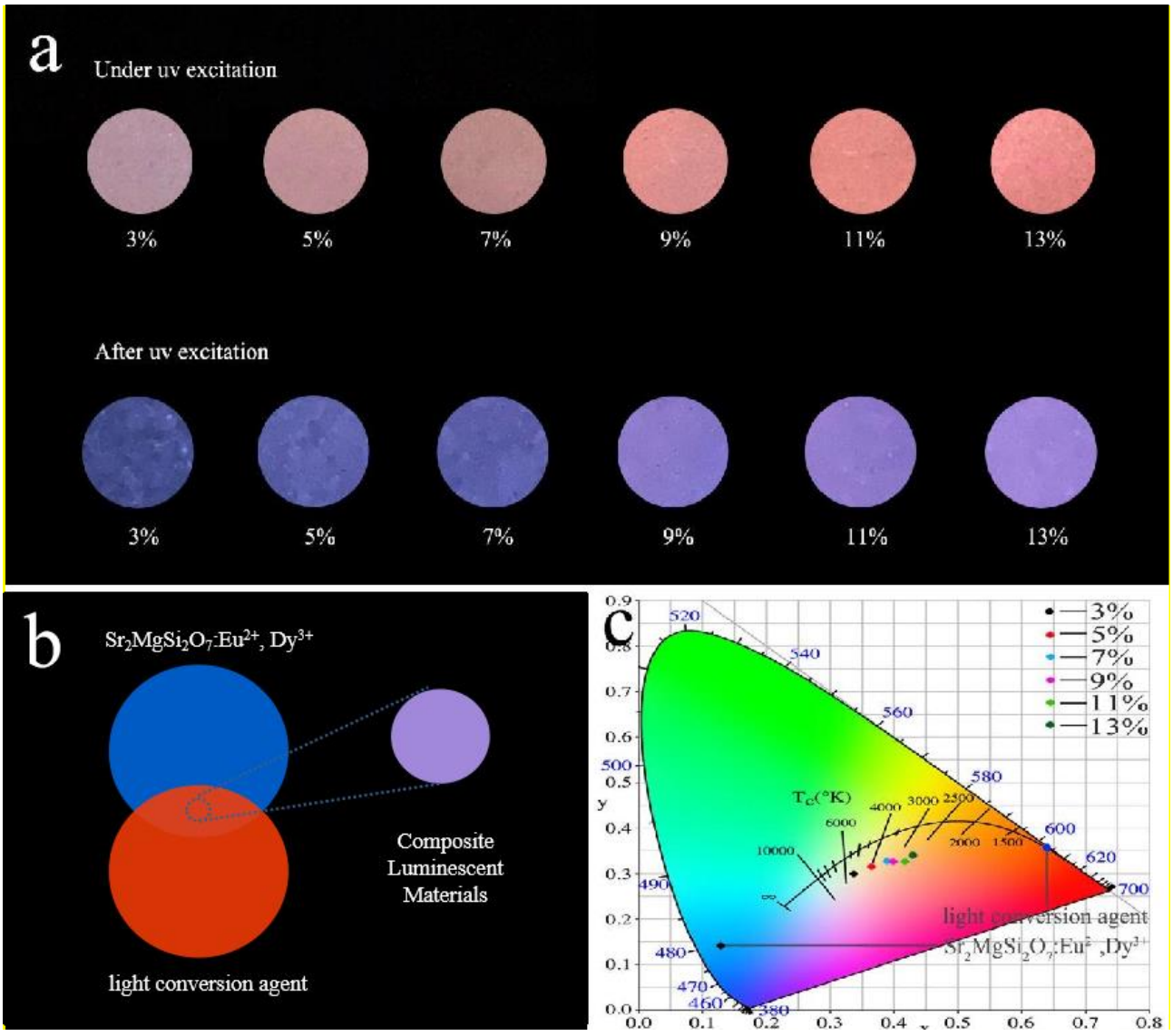

Fig. 7. (a) Digital pictures of the luminescent films subjected to UV excitation (365nm) and after the UV irradiation (365 nm) was stopped for 5 min; (b) Digital pictures of $Sr_2MgSi_2O_7:Eu^{2+}$, Dy^{3+}, light conversion agents and composite luminescent materials subjected to UV excitation (356 nm). (c) CIE chromaticity diagram of luminescent films with varying amounts of luminescent materials (3%, 5%, 7%, 9%, 11%, and 13%) (color online)

2.6. Colorimetric analysis

In Fig. 7 (a), the luminescent films, observed under and after UV excitation in the dark, with different amounts of the composite luminescent materials are demonstrated. The visible color of the samples gradually starts exhibiting the color red when the content of the composite luminescent materials is increased from 3% to 13%. The samples appear red under conditions of UV excitation and blue when not subjected to UV irradiation. Above results should be attributable to the varying ratios of red and blue light emitted from samples. As the light conversion agent is a type of instant luminescent material, it converts blue light of $Sr_2MgSi_2O_7:Eu^{2+}$, Dy^{3+} into red light under UV excitation. Only blue light from $Sr_2MgSi_2O_7:Eu^{2+}$, Dy^{3+} is emitted when the UV excitation stops. Thus, the greenhouse film containing composite luminescent materials, such as $Sr_2MgSi_2O_7:Eu^{2+}$, Dy^{3+}/light conversion agent, are capable of replenishing varying ratios of both red and blue light at daytime and nighttime.

White light is made up of seven colors. These colors are the components of the color reflected as luminescence light by luminescent materials individually or in combination with each other. The color of the light emitted by a composite material is composed of the blue light of $Sr_2MgSi_2O_7:Eu^{2+}$, Dy^{3+} and red light of light conversion agent (Fig. 7 (b)). Light color of the greenhouse film can also be adjusted by adjusting the ratio of $Sr_2MgSi_2O_7:Eu^{2+}$, Dy^{3+} and the light conversion agent. Corresponding color coordinates in the luminescent films contain 3%, 5%, 7%, 9%, 11%, and 13% luminescent materials (Fig. 7 (c)).

3. Conclusions

A type of luminescent plastic film was prepared, which can absorb UV or near-UV light and transformit to red and blue light that plants require for growth via functional particle $Sr_2MgSi_2O_7:Eu^{2+}$, Dy^{3+} as well as light conversion agents. This film is capable of storing energy during the day. The stored energy can be used to emit red and blue lights at night. The afterglow initial brightness of a luminescent film can reach up to 186.4 mcd/m^2, and the afterglow emission may last for over 8 hours. The emission spectrum of the luminescent film with 356 nm as the exciting wavelength shows two emission peaks at about 470 and 600 nm. This finding indicates that the studied film can provide red and blue light to plants; thus, addressing the pertaining agriculture issues. The intensity ratio of the red and blue light released by the film can be adjusted by introducing different amounts of composite luminescent materials.

Acknowledgement

This research gained sponsorship from Natural Science Foundation of Jiangsu Province (BK20171140, BK20180629), National Natural Science Foundation of China (51803076).

References

[1] C. Kami, S. Lorrain, P. Hornitschek, C. Fankhauser, Plant Development **91**, 29 (2010).
[2] X. Jing, H. Wang, B. Gong, S. Liu, M. Wei, X. Ai, Y. Li, Q. Shi, Plant Physiol. Biochem. **124**, 77 (2018).
[3] R. Sasidharan, C. Chinnappa, M. Staal, J. Elzenga, R. Yokoyama, K. Nishitani, L. Voesenek, R. Pierik, Plant Physiol. **154**(2), 978 (2010).
[4] M. Rehman, S. Ullah, Y. Bao, B. Wang, D. Peng, L. Liu, Environmental Science and Pollution Research **24**(32), 24743 (2017).
[5] S. Hogewoning, G. Trouwborst, H. Maljaars, H. Poorter, W. Van Ieperen, J. Harbinson, Journal of Experimental Botany **61**(11), 3107 (2010).
[6] A. Savvides, D. Fanourakis, W. Van Ieperen, Journal of Experimental Botany **63**(3), 1135 (2012).
[7] A. Centofante, Scientia Horticulturae **259**, 108765 (2020).
[8] Q. Ying, Y. Kong, C. Jones-Baumgardt, Y. Zheng, Scientia Horticulturae **259**, 108857 (2020).
[9] R. Wojciechowska, A. Kolton, O. Dlugosz-Grochowska, E. Knop, Scientia Horticulturae **211**, 179 (2016).
[10] Y. Miao, Q. Chen, M. Qu, L. Gao, L. Hou, Scientia Horticulturae **257**, 108680 (2019).
[11] S. Lee, J.-W. Park, Sensors and Actuators B-Chemical **298**, 126883 (2019).
[12] B. Chi, X. Zhang, Q. Shi, N. Wang, Y. Liu, International Journal of Pest Management **65**(4), 338 (2019).
[13] X. Wang, G. Wang, J. Li, Z. Liu, W. Zhao, J. Han, Chemical Engineering Journal **336**, 406 (2018).
[14] L. Miao, Y. Zhang, X. Yang, J. Xiao, H. Zhang, Z. Zhang, Y. Wang, J. Jiang, Food Chem. **207**, 93 (2016).
[15] B. He, Y. Chen, H. Zhang, C. Xia, Q. Zhang, W. Li, Horticulture Environment and Biotechnology **59**(4), 519 (2018).
[16] P. Gautam, M. Terfa, J. Olsen, S. Torre, Scientia Horticulturae **184**, 171 (2015).
[17] W. Chen, Y. Wang, W. Zeng, S. Han, G. Li, H. Guo, Y. Li, Q. Qiang, New Journal of Chemistry **40**(1), 485 (2016).
[18] Y. Zhu, Z. Pang, J. Wang, M. Ge, S. Sun, Z. Hu, J. Zhai, J. Gao, F. Jiang, Journal of Rare Earths **34**(5), 483 (2016).
[19] Y. Zhu, Z. Pang, J. Wang, M. Ge, A. Ju, Journal of Materials Science: Materials in Electronics **27**(7), 7554 (2016).
[20] X. Zhang, Z. Zhou, F. Ye, X. Liu, Q. Li, Materials Science in Semiconductor Processing **40**, 130 (2015).
[21] H. Xue, Z. He, X. Shen, Y. Zhu, M. Ge, Journal of Materials Science: Materials in Electronics **29**(21), 18045 (2018).
[22] J. Zhang, Y. Zhang, J. Tao, Y. Sun, Y. Zhu, Journal of Materials Science: Materials in Electronics **29**(13), 10762 (2018).
[23] Y. Xia, H. Ou, W. Li, G. Han, Z. Li, Nanomaterials **8**(4), 260 (2018).

*Corresponding author: zhuyanan@jiangnan.edu.cn